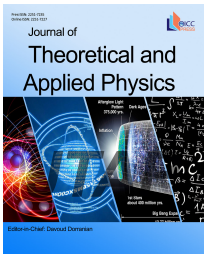

Volume 19, Issue 2, 192519 (1-10)

Journal of Theoretical and Applied Physics (JTAP)

https://doi.org/10.57647/j.jtap.2025.1902.19

First study on lattice potential energy determination from ultrasonic mean sound velocity for polycrystalline $Ca_{1+x}Cu_{3-x}Ti_4O_{12}$ perovskites and mono-crystalline counterparts

Dolly J. Parekh[1], Drashti K. Thummar[1], Nirali S. Kanani[1], Nimish H. Vasoya[2], Kunal B. Modi[1,*]

[1]*Department of Physics, Saurashtra University, Rajkot, India.*
[2]*Department of Toy Innovation, Centre of Toy Science, Children's Research University, Gandhinagar, India.*

[*]**Corresponding author:** kunalbmodi2003@yahoo.com

Original Research

Received:
27 November 2024
Revised:
6 February 2025
Accepted:
2 April 2025
Published online:
10 April 2025

Abstract:

For the first time the lattice energies (U_{LP}) for multi-crystalline specimens of perovskite system, $Ca_{1+x}Cu_{3-x}Ti_4O_{12}$ with $x = 0.0 - 1.0$, have been calculated using mean sound velocity data by employing Kudriavtsav's approach. The observed decrease in U_{LP} as a function of Ca^{2+} substitution has been described considering the structural and microstructural parameters. Using four different estimation models lattice energy (U_{LS}) values for mono–crystalline counterparts have been calculated. The difference between U_{LP} and U_{LS} ($U_{LS} > U_{LP}$) has been discussed based on grain boundary and grain contribution and the existence of voids and micro-cracks in multi-crystalline ceramics. A straightforward method proposed to determine U_{LS} for multi-cationic oxide systems founded on the oxide additivity rule was adequate.

Keywords: Lattice potential energy; Ultrasonic mean sound velocity; Structural and microstructural parameters; Oxide additivity rule

1. Introduction

Calcium-copper-titanate ($CaCu_3Ti_4O_{12}$) belongs to the quadruple perovskites with the general formula, $AA'_3B_4O_{12}$. The crystallographic sites, the dodecahedral (A-) sites, square-planner (A'-) sites, and octahedral (B-) sites, correspond to cubic perovskite structure (space group Im3 No. (204) and point group T_h) [1, 2]. For more than two and half decades pure and substituted calcium-copper-titanate ($CaCu_3Ti_4O_{12}$)- based materials and their isostructural systems have been extensively researched for potential use in a wide range of applications. Materials may be in single crystalline, polycrystalline, nanocrystalline, nanocomposites, thin film forms. They were found suitable for promising applications such as supercapacitors, varistors, gas-sensors, humidity sensors, photocatalytic and photoelectrochemical materials, rectification etc., [3]. From the fundamental research point of view, understanding the nature and the factors that affect binding forces within polycrystalline materials through elastic properties and lattice energy helps in deciding the applicability of the material for a specific application [4].

In ionic solids, the bond strength is measured by the lattice potential energy (U_L) value. The characteristics, reactivity, and structure of solids are elucidated by this lattice energy. The U_L is mentioned as a prominent parameter for the manifold thermodynamic evaluation of steadiness and the existence of intricate ionic alloys. It is a very tough task to determine U_L experimentally. This is because the crystalline material is set apart into atoms and not into gaseous ions, as needed in the U_L determination. Of course, the Born-Haber-Fajans thermodynamic cycle [5] can be employed using supplementary thermodynamic data,

to determine an experimental value of U_L. Consequently, in the area of contemporary materials science, alternate ways of experimental determination of U_L or theoretical computation of U_L are subjects of prime attentiveness. At the outset of the 1990s, many theoretical estimation methods such as the Born-Lande and Born-Mayer equations (https://en.wikipedia.org/wiki/Ionization_energy) are available in the literature that can be used to determine U_L. The limitation of these methods is that they apply to binary ionic solids only. Later on, in 1956 Kapustinskii [6] developed an equation that allows the evaluation of U_L for any simple ionic crystal. This expedites a path for spanning the evaluation of U_L to several scientific studies [7]. Because of the complexity of inorganic compounds, hardly any research articles on the Quantitative Structure Property Relationship (QSPR) are available. Earlier, Mu et al. [8] designed a few QSPR models with the aid of several model parameters to approximate the lattice energy values of ionic compounds. The recent calculation methods need particulars regarding the cell edge parameters, the coordination number of ions as well as force field. During the explicit lattice potential energy computation process [9] solid's lattice energy is produced in the course of its modeling. Besides, the determination of U_L from the quantum mechanical procedure is cumbersome and thus worthy for the simpler systems only. On the contrary, in the literature, several exceptionally expeditious methods for the determination of U_L of ionic crystals are available. This includes (i) Kapustinski's equation [6] relies on ionic charge and radii of ions involved (ii) Glasser and Jenkins model [9] based on the ionic strength (iii) lattice energy determination from connectivity and converse indices given by Mu et al. [8] (iv) determination of lattice- potential energy from chemical hardness proposed by Kaya and Kaya [10], and (v) Oxide additivity rule founded on the work of Shanon et al. [11]. The implementation of these models is relatively easy. These five distinct theoretical models have been employed in the present investigation. Besides, there are many other models available in the literature used to determine lattice potential energy (U_{LS}) for single crystalline materials including Born–Mayer, Varshani-Shukla and L_5 (logarithm) models [12]. The determination of U_{LS} from the quantum mechanical procedure is cumbersome and thus worthy for the simpler system only. The empirical method based on the chemical bond theory proposed by Liu et al. [13] requires detailed crystallographic information and elaborate computation. These models are hinged on atom-atom pair potential calculations and atomistic computational modelling [14]. In short, implementation of such models is not straightforward for complex/multi-cationic oxide systems as in the present case.

Unexpectedly, in the literature, very few reports are available on the lattice energy value of polycrystalline oxide systems for comparison. Subrahmanyam et al. [15] reported the lattice energies of NaCl-structured alkaline earth oxides, MgO ($U_{LP} \approx -24.61$ eV) and SrO ($U_{LP} \approx -20.21$ eV). Besides, for alkali fluorides, CaF_2 ($U_{LP} \approx -23.32$ eV), BaF_2 ($U_{LP} \approx -20.73$ eV), and $CdFe_2$ ($U_{LP} \approx -29.28$ eV) lattice energy values are reported. They all are multi-crystalline. By, contrast lattice energies for their monocrystalline counterpart (U_{LS}) are found to be -39.33 eV for MgO, -33.34 eV for SrO, -27.47 eV for CaF_2, -24.26 eV for BaF_2 and -30.44 eV for CdF_2 [9]. It is concluded that $U_{LS} > U_{LP}$ is for different reasons. Quantum mechanically calculated lattice energies for a large number of ABO_3-type perovskite compositions where A = trivalent La, Tb, Ce, Dy, Nd, Ho, Sm, Er, Eu, Pr, Nd, Yb, Gd, Lu, and B = trivalent Al, Cr, Fe, Ga, In and Sc are reported by Levy [16]. Accordingly, the lattice energy is weakly structure sensitive and a large value of lattice energy suggests better structural stability. A few years back, the lattice potential energies of a total of 38 polycrystalline oxide compositions of spinel ferrites, garnets, superconductors, and manganite perovskites were determined. The U_L of monocrystalline counterparts was calculated using four estimation models [17]. Zhang and his co-workers [18–24] carried out a study on the lattice potential energy of different cation-anion bonds (not the lattice energy of the composition as a whole) present in a large class of ceramics, ZnZr $(Nb_{1-x}R_x)_2O_8$ (R = Ta, Sb) (x = 0.02, 0.04, 0.06, 0.08 and 0.10), Nd $(Nb_{1-x}Sb_x)_2O_4$ (x = 0.00, 0.02, 0.04, 0.06, 0.08 and 0.10), $Ca_{1-x}Sr_xWO_4$ (x = 0.00, 0.02, 0.04, 0.06, 0.08 and 0.10), La $(Nb_{1-x}Ta_x)O_4$ ($x = 0.00 - 0.10$), $MgZrNb_{2+x}O_{8+2.5x}$ ($-0.08 \leq x \leq 0.08$), $(Nd_{1-x}La_x)$ NbO_4 and $LaNbO_4$, based on complex bond theory. Similar investigations have been performed on lattice energy determination of bonds involved in ceramic materials, $BaCu_{2-x}Co_xSi_2O_7$ [25], Ta-substituted 0.15ZnO-0.15Nb_2O_5-0.55TiO_2 [26] and $Ba_{1-x}Sr_xCu_2Si_2O_7$ [27].

It is intriguing to investigate the substitution effect of large cations, for example, Ca^{2+} ions with an ionic radius equal to the threshold value ~ 1 *Å* for Cu^{2+} (0.73 *Å*) in the $CaCu_3Ti_4O_{12}$. Thus, structural properties are expected to influence to a greater extent. Secondly, the replacement of paramagnetic (magnetic moment 1 μ_B) Jahn–Teller Cu^{2+} ions with non–magnetic Ca^{2+} ions in the series, $Ca_{1+x}Cu_{3-x}Ti_4O_{12}$ expected to affect magnetic properties as well. In short, the substitution of Ca^{2+} ions for Cu^{2+} ions eventually influences other physical properties. The ionic radius of Ca^{2+} ions is too large compared to the ionic radius of Cu^{2+} ions. Thus, there is a substitution or accommodation limit in the crystallographic structure without disturbing the cubic perovskite structure of pristine $CaCu_3Ti_4O_{12}$ (space group Im3 No. (204) and point group T_h). Earlier we found that in the investigated series, $Ca_{1+x}Cu_{3-x}Ti_4O_{12}$ x = 0.0, 0.1, and 0.2 compositions possess single-phase structures. Besides x = 0.5 and 1.0 compositions are bi-phasic. They possess respectively $\sim$ 83% and 77% of the $CaCu_3Ti_4O_{12}$ phase and $\sim$ 17% and 23% of orthorhombic $CaTiO_3$-phase [2]. According to the literature $Ca_2Cu_2Ti_4O_{12}$ (x = 1.0) composition of the series, $Ca_{1+x}Cu_{3-x}Ti_4O_{12}$, demonstrates mixed-phase characteristics [28, 29]. The composition possesses $\sim$ 67% of $CaCu_3Ti_4O_{12}$ cubic perovskite phase and $\sim$ 33% of orthorhombic $CaTiO_3$ phase. Our finding is consistent with the reported one. Interestingly, x = 2.0 composition, $Ca_3CuTi_4O_{12}$, exhibits a mono-phase cubic perovskite structure similar to that of $CaCu_3Ti_4O_{12}$ (x = 0.0) composition. The extreme composition of the series, $Ca_4Ti_4O_{12}$, with x = 3.0 is fundamentally nothing but 4 × $CaTiO_3$ with

a single-phase orthorhombic structure. Thus, there is no substitution limit except phase change and its influence on various physical properties.

Till today determination of lattice potential energy for ionic crystals is an important area of research. As far as we know, no research reports on lattice energies of multi-crystalline and mono-crystalline quadruple perovskite systems in general and $Ca_{1+x}Cu_{3-x}Ti_4O_{12}$ series with $x = 0.0$, 0.1, 0.2, 0.5, and 1.0, in particular, are available in the literature. No details are accessible on the comparative investigation deals with the lattice potential energy of multi-crystalline (U_{LP}) oxides and their mono-crystalline (U_{LS}) counterparts, the factors influencing U_L, and the factors causing the difference between the two (U_{LP} and U_{LS}).

In the recent past, we have investigated the distribution of cations, and the evolution of magnetic ordering in $Ca_{1+x}Cu_{3-x}Ti_4O_{12}$ ($x = 0.0 - 1.0$) perovskites [1]. The defect structural modifications in $Ca_{1+x}Cu_{3-x}Ti_4O_{12}$ have been investigated by positron annihilation lifetime spectroscopy and supplementary techniques [2]. The electron spectroscopy for chemical analysis was employed to explore the impact of Ca^{+2}- substitution on the electronic structure of $CaCu_3Ti_4O_{12}$ [30]. Very recently, we have investigated the elastic properties of $Ca_{1+x}Cu_{3-x}Ti_4O_{12}$ ($x = 0.0 - 1.0$), by ultrasonic pulse echo selection technique [4].

The dearth of systematic in-length lattice potential energy determination studies on pure and substituted quadruple perovskite $CaCu_3Ti_4O_{12}$ stimulates the present investigation. The principal objective of the current study is to figure out the lattice energy values for the polycrystalline oxide series, $Ca_{1+x}Cu_{3-x}Ti_4O_{12}$ ($x = 0.0 - 1.0$), whose lattice potential energies have not been cited. Based on Kudriavtsev's theory, an average sound velocity resolute by employing an ultrasonic pulse-echo selection method and corrected to the void-free state [4] has been used to calculate the lattice potential energies (U_{LP}) of polycrystalline ceramics. Four different theoretical and semi-empirical approaches have been used to calculate lattice energies of monocrystalline (U_{LS}) counterparts. The difference observed between the two, U_{LP} and U_{LS}, has been explained in length. Eventually, the suitability of the oxide additivity rule for U_{LS} determination has been examined.

2. Experimental details

In our preceding reports [1, 2, 30] the experimental particulars regarding the fabrication of five multi-crystalline specimens of $Ca_{1+x}Cu_{3-x}Ti_4O_{12}$ system with $x = 0.0$, 0.1, 0.2, 0.5, and 1.0, through standard double sintering solid state reaction route are well discussed. This synthesis technique is easy to operate with the advantages of simple processes such as synthesis, high yield, high selectivity, high purity, uniform particle size distribution, controllable size, high potential for scalability, possibility for tonnage production and less pollution (minimum waste generation due to no solvent usage). Further, this technique can synthesize materials with unique properties that may not be achievable through solution-based methods (soft-chemical routes). Finally, said method is particularly suitable for the preparation of complex and multi-cationic oxide systems. The Rietveld refined X-ray diffraction profiles indicate that the compositions with $x = 0.0 - 0.2$ retain mono-phasic characteristics whilst the compositions with $x = 0.5$ and 1.0 have mixed–phase characteristics. They possess $CaCu_3Ti_4O_{12}$ as a primary phase and $CaTiO_3$ as a secondary phase in different proportions. The structural parameters, molecular weight (M_W), lattice constant a (nm), molecular volume (V_m), and X-ray density (ρ_x), thus determined are summarized in Table 1 to facilitate the further discussion on the dependence of lattice energy on Ca^{2+}-content in the system. Besides, the technical details of the ultrasonic pulse-echo selection technique are described in [31]. The measurements are carried out at $T = 300$ K by keeping the frequency of the transducer, $f_a = 1$ MHz.

3. Results and discussions

The values of the lattice parameter, a (nm), hence resolved are in turn used to compute the unit cell volume, $V_{\text{cell}} = a^3$ (nm^3). The molecular volume, V_m, can be estimated from $V_m = V_{\text{cell}}/Z$, where Z is the number of unit cells per formula unit, i.e. $Z = 2$ for cubic perovskite structure. Besides, the ρ_x has been computed with the help of the standard formula: $\rho_x = M_W/(N_A \cdot V_m)$, where N_A is Avogadro's number given by 6.02×10^{23} molecules/mol. The computed values of V_{cell}, V_m and ρ_x for all the compositions are given in Table 1.

The velocity of longitudinal wave (V_l) and velocity of shear wave (V_s) determined experimentally for multi-crystalline bulk samples from ultrasonic pulse-echo selection techniques [31] are corrected to zero-porosity (V_{l0}, V_{s0}). These are further used to calculate the non-porous value of mean sound velocity using the known relation [32, 33], V_{m0} (m/s) $= [3(V_{l0}^3 \cdot V_{s0}^3)/(V_{s0}^3 + 2V_{l0}^3)]^{1/3}$, for the investigated compo-

Table 1. Molecular weight (M_W), molecular volume (V_m), X-ray density (ρ_x), meansound velocity (V_{m0}), and lattice energy (U_{LP}) (Kudrivatsav's theory) for polycrystalline compounds.

Ca^{2+}- concentration (x)	M_W (kg) $\times 10^{-3}$	a (nm)	V_m $(\text{nm})^3$	ρ_x (g/cm^3)	V_{m0} (m/s)	-U_{LP} (eV)
0.0	614.33	0.73965(5)	0.2023	5.043	1700.7	552.25
0.1	611.98	0.74074(2)	0.2029	5.001	1627.3	503.67
0.2	609.64	0.74228(8)	0.2045	4.950	1540.9	449.88
0.5	602.60	0.73770(10)	0.2007	4.824	1495.9	419.13
1.0	590.86	0.73809(22)	0.2010	4.686	1535.2	432.75

sitions, $x = 0.0$, 0.1, 0.2, 0.5, and 1.0 of $Ca_{1+x}Cu_{3-x}Ti_4O_{12}$ series. Table 1 summarizes these values.

3.1 Determination of lattice potential energy from V_{m0} for multi-crystalline materials

Founded on Kudrivatsav's theory [34] and using the V_{m0} data, the lattice potential energy values of various ionic crystals have been computed successfully. The theory was found successful in approximating the lattice energy of divalent metal chalcogenides even if sufficient covalency is present [15]. Earlier, the temperature depends on the lattice energy of AB_2– type crystals, alkali halides, alkaline earth oxides, ammonium bromide, heavy metal halides, and ammonium chloride were investigated [15], and not only that, details concerning to change of phase were obtained. A few years ago, this theory was employed to evaluate the lattice energy of various polycrystalline oxide systems [32, 33, 35, 36].

Following Kudrivatsav's theory, supposing the additivity of internal energy depends on temperature (T (K)), M_W (kg), and potential energy (U_0 (eV)) of the material, is stated by

$$V^2 = -\frac{nm\gamma}{U_0} + \frac{\gamma RT}{M} \tag{1}$$

where the constants, n, and m, signifying that the potential energy function relies on the lattice structure, γ serves as the ratio of molecular heat capacities (C_P/C_V), (for the majority of the ionic solids, γ is roughly equal to unity) and R is the gas constant. In equation (1) for ionic solids, U_0 can be put back by the lattice potential energy of the polycrystalline material (U_{LP}), the $\eta = 3$ settles worthy for numerous spinel structured ferrites, crystals with *bcc* garnet structure, and several solids [32, 33, 35, 36].

Taking the above points into consideration, lattice energy (U_{LP}) in its simplistic form is presented by:

$$U_{LP}\,(\text{eV}) = -3.108(M_W \cdot V_{m0}^2) \times 10^{-5} \tag{2}$$

where V is replaced by V_{m0} (Table 1). In Table 1 the U_{LP} values calculated for the investigated samples are also included. Customarily, the lattice energy of a crystalline solid is defined as the crystal formation energy from infinitely separated ions, and as a consequence, the lattice energy is always negative.

At this point, it would be engrossing to study the variation of U_{LP} with Ca^{2+}- content (x). The elastic constants and their pressure derivatives are evocative of the short-range contribution to the U_L. Thus, the factors tailoring the magnitude of elastic constants are also indirectly responsible for governing the strength of bonding (i.e., lattice energy). We have attempted to describe the variation of lattice potential energy as a function of Ca^{2+}- substitution (x) in the best possible way considering the different structural and microstructural parameters.

It is well-established fact that the non-magnetic metallic cations with an entirely filled outermost orbit such as Li^{1+} ($1s^2$), Mg^{2+} ($2p^6$), Ga^{3+} ($3d^{10}$), etc., are highly stable as compared to the highly magnetic cations with a half-filled outermost orbit like Fe^{3+} ($3d^5$) and Mn^{2+} ($3d^5$) as well as cations having incomplete or partially filled outermost orbit such as Co^{2+} ($3d^7$), Cr^{3+} ($3d^3$), Mn^{4+} ($3d^3$), etc. [17, 37]. In the series, $Ca_{1+x}Cu_{3-x}Ti_4O_{12}$, magnetic Cu^{2+} ($S = 1/2$, 1 μ_B) ions with the partially filled outermost orbit ($3d^9$) are replaced by non-magnetic Ca^{2+} (0 μ_B) ions with the filled outermost orbit ($3p^6$) and that do not participate in active bonds formation. Besides, the replacement of Cu^{2+} ion with ionic radios of 0.73 *Å* by quite larger Ca^{2+} ion having an ionic radius of 1.00 *Å* gives rise to lengthened bond–length that weakens the bond strength. Consequently, combining the above two aspects, with Ca^{2+}- substitution in the system, U_{LP} is expected to fall off.

The observed enhancement in lattice energy (U_{LP}) value for $x = 1.0$ composition can be described as follows. Earlier, Solunke et al. [38] reported that Ag^{1+} ions doped in Bi–2212 superconducting series, inhabit the grain boundaries. Later on, according to Rajmi et al. [39] in $MgTiO_3$-doped $CaCu_3Ti_4O_{12}$ materials, $MgTiO_3$ inhabits at the grain boundary and contributed to the inter-grain strengthening effect. In the present system also secondary $CaTiO_3$– phase is supposed to reside at the grain boundary. This is anticipated to obstruct dislocation motion (strain). Thus, the inter-atomic bonding strength (lattice energy) is enhanced as observed.

de Boer et al. [40] referring to the AB_2O_4– type ferrites showed that the electrostatic share to the lattice energy is increased for ferrites in which the octahedral (B-) site is occupied with different metallic cations (inverse spinels) (e.g. $NiFe_2O_4$) as compared to ferrite materials in which the B- site is occupied by only one type of cation (normal spinels) (e.g. $ZnFe_2O_4$). On a similar line of argument, in the series under investigation, $Ca_{1+x}Cu_{3-x}Ti_4O_{12}$, for a pristine composition ($x = 0.0$), A, A', and B- sites are fully occupied by only one type of cation such as Ca^{2+}, Cu^{2+}, and Ti^{4+} respectively. With Ca^{2+} on Cu^{2+}- site (A'-site), for $x = 0.1$ and $x = 0.2$ compositions A'– site is occupied by three distinct cations, Ca^{2+}, Cu^{2+}, and Ti^{4+}, with different concentrations, and on the B-site along with the majority of Ti^{4+}- ions small amount of Cu^{2+}- ions are also present. Besides, for $x = 0.5$ and 1.0 compositions, Ca^{2+}, and Cu^{2+}, ions reside the A'- site while the B-site is fully occupied by Ti^{4+} ions only. Thus, for $x = 0.1$ to 1.0 compositions electrostatic contribution and accordingly lattice energy value should increase as compared to the parent composition. But this is not the case. It seems that in the present study electrostatic contribution is not a governing factor or contribution may be insignificant to the lattice potential energy value. Similarly, based on a careful study, it also concluded that the grain size reduction, 4.9 μm ($x = 0.0$) to 4.2 μm ($x = 0.2$) and decrease in porosity value, 23.12% ($x = 0.0$) to 9.2% ($x = 0.5$) [20, 24] are also not deciding parameters to the lattice energies. In our previous study [17] all these three factors were found important in explaining the compositional dependence of lattice energy values for different oxide systems.

3.2 Determination of lattice potential energy with the help of Kapustinskii's equation

When comprehensive structural data of an ionic crystal is not available, the lattice potential energy (U_{LS}) can be de-

termined from Kapustinskii's equation [6]. Besides, experimental determination of U_{LS} is quite difficult. This approach is referred to as the most successful for estimating the lattice energy values for an extensive range of ionic crystals. The factors (i) thermo-chemical radii, wherein the ions are regarded as a sphere of the bonded ions, and (ii) the charge of the ion, contribute to the magnitude of U_{LS}. Accordingly, U_{LS} in terms of cationic charge (Z^+), anionic charge (Z^-), the cationic radius (r^+), the radius of the anion (r^-) and q, the number of ions in the chemical formula (i.e. $q = 20$ for $Ca_{1+x}Cu_{3-x}Ti_4O_{12}$ series) is given by:

$$U_{LS} = -1202.5 \times q \times \frac{|Z^+||Z^-|}{r^+ + r^-} \times \left[1 - \frac{0.345}{r^+ + r^-}\right] \quad (3)$$

The r^- is 1.32 Å while Z^- is (−2) for oxygen anion. To calculate r^+ and Z^+, we have considered the weighted average of ionic radii and ionic charge of cations involved in the composition. Before applying Kapustinskii's equation for the determination of U_{LS} values for the different compositions of the series, $Ca_{1+x}Cu_{3-x}Ti_4O_{12}$, the validity of this equation has been tested by calculating the U_{LS} values for the related compounds whose lattice energy values are available in the literature. The comparison is made between computed values and reported values. Based on atomistic simulations, Mather et al. [41] reported a lattice energy value (−150.88) eV per formula unit for $CaTiO_3$. Besides, based on atomistic computer simulation Donnerberg and Catlow [42] determined a lattice energy value of (−142.5) eV for a monocrystalline $YFeO_3$ compound while for $Y_4Fe_4O_{12}$ the value is reported to be (−567.6) eV. The lattice potential energy values calculated based on equation (3) are found to be (−147.52) eV for $CaTiO_3$, (−149.82) eV for $YFeO_3$, and (−599.27) eV for $Y_4Fe_4O_{12}$. A reasonable agreement between the two is seen. This confirms the validity and allows the applicability of Kapustinskii's equation for lattice energy determination for the perovskite series under study. Further, compared to the lengthy computer simulation process this methodology proved to be straightforward for lattice energy determination. The values of U_{LS} thus obtained for $x = 0.0 - 1.0$ compositions are in kJ/mol, however, for comparison purposes, they are given in eV (Table 2).

3.3 Lattice potential energy determination for complex ionic solids

According to Glasser and Jenkins [9] the limiting relations given below can be used to calculate the U_{LS} of complex ionic solids.

$$U_{LS} = AI\left(\frac{2I}{V_m}\right)^{\frac{1}{3}} \quad (4)$$

$$U_{LS} = AI\left(\frac{\rho_x \times N_A \times 2I^4 \times A^3}{10^{21} \times M_W}\right)^{\frac{1}{3}} \quad (5)$$

where A is a usual term of electrostatic conversion having a value equal to 121.39 kJ/mol/nm, the factor 10^{21} is used to convert cubic nanometers to cubic meters and I is the term related to the ionic strength is defined as:

$$I = \frac{1}{2}\sum(n_i Z_i^2) \quad (6)$$

Here n_i is the number of ions of type i per formula unit and Z_i is the corresponding charge. The summation is extended over all ions involved in the formula unit.
For instance, I for $x = 0.5$ composition ($Ca^{2+}_{1.5}Cu^{2+}_{2.5}Ti^{4+}_4O^{-2}_{12}$) of the series, $Ca_{1+x}Cu_{3-x}Ti_4O_{12}$, can be calculated as:

$$I = \frac{1}{2}[1.5(2)^2 + 2.5(2)^2 + 4(4)^2 + 12(2)^2] = 64 \text{ (Table2)}$$

For all the compositions I is going to remain the same as Ca and Cu possess the same ionic charge of +2. In Table 3 U_{LS} values calculated for all the compositions are depicted.

3.4 Determination of lattice potential energy from connectivity and converse indices

Ionic crystals possess anions as well as cations and strong interactions take place between these nearest negative and positive ions. The lattice energy contribution chiefly comes out from these interactions. The sum of lattice energies of those interacting ion pairs is influenced by factors such as electro-negativity (X_i), ionic radius (r_i), and ionic charge (q_i). According to Mu et al. [8], g_i, the ionic polarization force parameter is defined as:

$$g_i = \left[\frac{(1 + q_i^{1.7})(X_i)^{0.3}}{1 + r_i}\right] \quad (7)$$

It is important to note that g_i will be different for ions of different atoms and ions of the same atom with different charges. The values of X_i, q_i, r_i, and g_i for different ions under investigation are included in Table 4.
Centered on the adjacency matrix of molecular graphs, the connectivity index (^mG) and its converse index ($^mG'$) are described in this way [8]:

$${}^mG = \sum(g_i \cdot g_j \cdot g_k \cdots)^{0.5} \quad (8)$$

Table 2. The aggregate radius of the cations (r^+_{av}), cationic charges (Z^+_{av}), and lattice energies (U_{LS}) (Kapustinskii's equation) for $Ca_{1+x}Cu_{3-x}Ti_4O_{12}$ quadruple perovskite series.

Ca^{2+}- concentration (x)	r^+_{av} (Å)	Z^+_{av}	$-U_{LS}$ (eV)
0.0	0.70	3	613.66
0.1	0.71	3	612.79
0.2	0.71	3	609.80
0.5	0.72	3	609.56
1.0	0.74	3	605.56

Table 3. Computed values of I and U_{LS} (Glasser and Jenkins model for complex ionic solids) for $Ca_{1+x}Cu_{3-x}Ti_4O_{12}$ system.

Ca^{2+}- concentration (x)	I	$-U_{LS}$ (eV)
0.0	64	691.24
0.1	64	690.23
0.2	64	688.75
0.5	64	685.51
1.0	64	573.44

Table 4. Charge number (q_i), electro-negativity (X_i), ionic radius (r_i), and ionic polarization parameter (g_i) for different ions from connectivity and converse indices.

Element	$\|q_i\|$	X_i	r_i (Å)	g_i
Ca^{2+}	2	1.00	1.00	2.13
Cu^{2+}	2	1.90	0.73	2.98
Ti^{4+}	4	1.54	0.61	8.02
O^{2-}	2	3.44	1.32	2.65

$$ {}^{m}G' = \sum (g_i \cdot g_j \cdot g_k \cdots)^{-0.5} \tag{9} $$

where m is the order of the molecular connectivity index. The ${}^0G$, ${}^1G$, ${}^0G'$, and ${}^1G'$ are defined as follows:

$$ {}^0G = \sum (g_i)^{0.5} \tag{10} $$

$$ {}^1G = \sum (g_i \cdot g_j)^{0.5} \tag{11} $$

$$ {}^0G' = \sum (g_i)^{-0.5} \tag{12} $$

$$ {}^1G' = \sum (g_i \cdot g_j)^{-0.5} \tag{13} $$

In equations (10)-(13) $\sum$ is the sum of an atom of the composition and the sum of the chemical single bonds of the chemical formula. For each ion, the number of chemical single bonds bonding to other ions is equal to the charge numbers. In Table 5 ${}^0G$, ${}^1G$, ${}^0G'$, and ${}^1G'$ values for all the compositions are summarized. These values are further used to calculate U_{LS} applying the non-linear regression analysis-based model given by:

$$ U_{LS} = (-315.953) + 831.216({}^1G)^{0.896} + 44.576({}^0G)^{1.644} - 140.712({}^1G')^{2.150} + 110.096({}^0G')^{1.474} \tag{14} $$

In Table 5 lattice potential energies thus calculated are given. The values are unfairly sound agreement with those determined by employing alternative models.

3.5 Determination of lattice potential energy from the chemical hardness

Kaya and Kaya [10] demonstrate a novel method to determine U_{LS} for inorganic ionic crystals from chemical hardness. In the work, lattice energies of simple inorganic ionic compounds and alkali halides have been determined. According to density functional theory [43], chemical hardness (η) is the second derivative of electronic energy (E) concerning a number of electrons (N) at a constant external potential ($\upsilon(r)$) [44]. Thus,

$$ \eta = \frac{1}{2}\left(\frac{\partial^2 E}{\partial N^2}\right)_{\upsilon(r)} \tag{15} $$

The chemical hardness of molecules (η_M) can be calculated by the equation [10]:

$$ \eta_M = \frac{2\sum_{i=1}^{N} \frac{b_i}{a_i}}{\sum_{i=1}^{N} \frac{1}{a_i}} \tag{16} $$

In equation(16) N is the number of atoms present in the molecule, and the a_i and b_i parameters are delineated concerning ionization energy (I_E) and electron affinity (E_A) along these lines:

$$ \begin{aligned} a_i &= \frac{I_E + E_A}{2} \\ b_i &= \frac{I_E - E_A}{2} \end{aligned} \tag{17} $$

Table 5. Molecular weight (M_W), molecular volume (V_m), X-ray density (ρ_x), meansound velocity (V_{m0}), and lattice energy (U_{LP}) (Kudrivatsav's theory) for polycrystalline compounds.

Ca^{2+}- concentration (x)	${}^0G$	${}^1G$	${}^0G'$	${}^1G'$	$-U_{LS}$ (eV)
0.0	37.3839	94.8114	11.2516	6.4870	631.53
0.1	37.3571	94.7247	11.2623	6.5001	630.61
0.2	37.3303	94.6380	11.2729	6.5133	629.70
0.5	37.2499	94.3777	11.3049	6.5528	626.94
1.0	37.1159	93.9440	11.3581	6.6186	622.33

The equation for estimation of U_{LS} of ionic crystal in terms of η_M is given by:

$$U_{LS} = 2I\left[a\frac{\eta_M}{(V_m)^{1/3}} + b\right] \quad (18)$$

The constants a and b rely on the stoichiometry of the compound. The values of a_i and b_i have been estimated for constituent atoms, Ca, Cu, and Ti, considering the literature values of I_E and E_A into account (https://en.wikipedia.org/wiki/Ionization_energy, https://en.wikipedia.org/wiki/Electron_affinity). The η_M for all the compositions of the quadruple perovskite series, $Ca_{1+x}Cu_{3-x}Ti_4O_{12}$ have been evaluated considering the values of a_i and b_i (Table 6) adopting the calculating methodology discussed in [10]. The illustrative calculation of the un-substituted composition, $CaCu_3Ti_4O_{12}$ ($x = 0.0$), is given below.

$$\eta_{CaCu_3Ti_4O_{12}} = \frac{2[1\times\frac{3.0458}{3.0668}+3\times\frac{3.2466}{4.4796}+4\times\frac{3.3774}{3.4504}+12\times\frac{6.0795}{7.5405}]}{\frac{1}{3.0668}+\frac{3}{4.4796}+\frac{4}{3.4504}+\frac{12}{7.5405}} = 4.8554 \text{ eV} \quad (19)$$

It is worthwhile to note that the parameters a, b, and η_M located in equation(18) are related to the empirical constant α (which has a value close to that of A) and β discussed in [9]. The value of a so computed is ascertained 25 kJ/nm/mol/eV, whilst the b is settled to be ~ 248.18 kJ/mol for the pristine composition, $CaCu_3Ti_4O_{12}$ ($x = 0.0$). That was further used to calculate the U_{LS} of all other compositions and the same is included in Table 7. The values of U_{LS} are in accord with those computed based on other models. The inclusion of η influences extending the abscissa scale and a bit refines the correlation coefficient, making the new equation somewhat superior.

3.6 Oxide additivity rule

Earlier, Shanon et al. [11] successfully employed the oxide additivity rule to evaluate the electronic polarizability and dielectric polarizability of multi-cationic oxide composition. Later on, we extended the applicability of this rule to evaluate the lattice energy of spinel ferrites [17]. The relevancy of this rule for approximating the lattice energy values of the system under study has been tested. For the said purpose the lattice energy of constituent oxides [8], CaO, CuO, and TiO_2 (U_{LS} (CaO) = (−3401) kJ/mol, U_{LS} (CuO) = (−4050) kJ/mol and U_{LS} (TiO_2) = (−12054) kJ/mol are taken into account and according to [38]:

$$U_{LS}(Ca_{1+x}Cu_{3-x}Ti_4O_{12})(x = 0.0-1.0) = (1+x)U_{LS}(CaO) + (3-x)U_{LS}(CuO) + 4U_{LS}(TiO_2) \quad (20)$$

For example, U_{LS} for $x = 0.2$ ($Ca_{1.2}Cu_{2.8}Ti_4O_{12}$) composition can be calculated as:
U_{LS} ($Ca_{1.2}Cu_{2.8}Ti_4O_{12}$) ($x = 0.2$) = (1.2) U_{LS} (−3401 kJ/mol) + (2.8) U_{LS} (−4050 kJ/mol) + 4 U_{LS} (−12054 kJ/mol) = −63,637.2 kJ/mol = −659.53 eV (as 1 eV = 96.486 kJ/mol)
The lattice energy (U_{LS}) values for the studied compositions computed based on the above formula (20) are given in Table 8. The outcome is consistent with the U_{LS} values obtained from the other standard semi-empirical and theoretical models. In the literature no lattice potential energies determined experimentally or theoretically for multicrystalline and mono-crystalline $CaCu_3Ti_4O_{12}$ are available. Mather et al. [41] reported a lattice energy value (−150.88) eV per formula unit for $CaTiO_3$ based on atomistic simulations. Calcium-copper-titanate, $CaCu_3Ti_4O_{12}$, is a derivative of $CaTiO_3$. In 4 x $CaTiO_3$ (= $Ca_4Ti_4O_{12}$) when $3Ca^{2+}$ is replaced by an equal amount of Cu^{2+} that results in $CaCu_3Ti_4O_{12}$. Thus, one can expect a lattice energy value of 4 x (−150.88) eV (= −603.52 eV) for $CaCu_3Ti_4O_{12}$. This value of lattice energy is consistent with U_{LS} values determined from the different approaches with a $10-15\%$ variation. Furthermore, the lattice energy value for $CaTiO_3$ calculated using an oxide additivity rule is found to be (−160.17) eV matches well with the reported one. This advises that the oxide additivity rule can be a better option for cumbersome evaluation methods such as atomistic simulations as far as lattice energy determination has concerned. This also confirms the authenticity of the oxide additivity rule. The observed decrease in U_{LS} with concentration (x) suggests structural stability is distorted with Ca^{2+}- substitution. This finding is consistent with the finding of other characterizations. While lattice energies of complex oxide compounds are not at hand such methodology is very useful.
The examination of Tables 1, 2, 3, 5, 7, and 8 suggests that for all the compositions $U_{LS} > U_{LP}$. As discussed in section 1, this condition is observed for alkaline earth oxides and alkali fluorides [9, 15]. In the case of spinel-structured ferrite, *bcc*-structured garnets, superconductors, and manganite perovskites also the same relationship was found. This advises that the influencing factors to the lattice potential energy values of multi-crystalline materials and mono-crystalline counterparts are dissimilar and may be structure sensitive. Of course, the difference between U_{LS} and U_{LP} is relatively small for alkali fluorides while it is comparatively substantial for alkaline earth oxides. For the system under study, the difference between U_{LS} and U_{LP} is as small as 10% and as large as 25% depending on the model used.
The lower values of U_{LP} as compared to U_{LS} can be described along these lines. Multi-crystalline materials are

Table 6. Ionization energy (I_E), electron affinity (E_A), and a_i and b_i values for constituent atoms from Kaya and Kaya model based on chemical hardness.

Atom	I_E (eV)	E_A (eV)	a_i	b_i
Ca	6.1126	0.021	3.0668	3.0458
Cu	7.7261	1.233	4.4796	3.2466
Ti	6.8277	0.073	3.4504	3.3774
O	13.62	1.461	7.5405	6.0795

Table 7. The η_M and lattice potential energies (U_{LS}) values for all the compositions (Kaya and Kaya model based on chemical hardness).

Ca^{2+}- concentration (x)	η_M	$-U_{LS}$ (eV)
0.0	4.8554	604.00
0.1	4.8463	602.60
0.2	4.8372	601.52
0.5	4.8102	601.68
1.0	4.7662	599.05

made up of small crystals or grains that have different crystallographic arrangements and are segregated by a grain boundary. There is a certain kind of atomic inconsistency inside the region of grain boundary (which is possibly a few atomic distances wide) in a passage from the crystalline arrangement of one grain to that of a neighboring one. Among bordering grains, different degrees of crystallographic imperfect alignment are feasible. On the edge of the grain boundary, the atoms are bounded not so much as systematically as bound angles are longer and, accordingly there is a grain boundary energy or interfacial energy which depends on the order of misorientation, being larger for high-angle boundaries [45]. The long-distance interactions are restricted by these grain boundaries. Therefore, the lattice potential energy or strength of multi-crystalline material is lower than its mono-crystalline counterpart.

The lattice potential energy (U_{LP}) value ascertained from the average sound velocity is highly influenced not only by percentage porosity but also by morphology of pores (pore shape, pore size, the way pores are distributed, connectivity of pores, etc.) grain and grain boundary contributions, an isotropic thermal stress-produced occurrence and evolution of micro cracks, number of cracks per unit volume (crack-density), shapes of cracks (circular, long rectangular, ellipsoidal, etc.), as discussed [45]. According to Goktas and his co-workers [46] in polycrystalline manganites the grain boundary effects greatly influence their magnetoresistance properties. The exceedingly interrelated pores lead to a weakened structure. Besides, the valleys that form among grains will come up with sites of large stress concentrations and, therefore, large deformation. Conversely, pores with spherical shapes furnish large stiffness for a given porosity. At the same time, ellipsoidal-shaped pores tend to weaken a structure more than pores with spherical shapes caused by a combination of a less well-connected solid phase, and greater stresses and deformation near the high curvature regions of the ellipsoidal [45]. The oxygen content and related some sorts of defects also play a decisive role in controlling the bond strength (lattice energy). A short while ago, Shi et al. [47] investigated the influence of oxygen vacancy on bond ionicity, and lattice energy of Yb^{3+}- substituted CeO_2 ceramics. An oxygen vacancy within a crystal lattice directly affects the lattice energy by introducing structural distortion and disrupting the electrostatic interactions between ions, generally leading to a decrease in the overall lattice energy. The electronic structure study of $Ca_{1+x}Cu_{3-x}Ti_4O_{12}$ series ($x = 0.0 - 1.0$) employing X-ray photoelectron spectroscopy has demonstrated an observable shift for $x = 0.5$ and $x = 1.0$ compositions as compared to the compositions with $x = 0.0, 0.1, 0.2$. This shift could be partially attributed to the formation of oxygen vacancy defects [47] as evident from the positron annihilation lifetime and Doppler broadening spectroscopy measurements [2]. Thus, on increasing Ca^{2+}- substitution, oxygen vacancy increases result in a decrease in lattice energy as observed. When an oxygen atom is removed, the surrounding cations tend to relax inwards, creating a localized strain field that can affect the stability of the lattice. The upturn of the resistance observed at low temperatures (< 49 K) for LaBaMnO films produced by dip-coating on a quartz substrate was attributed to the strong structural disorder due to large lattice mismatch and strain relaxation [48]. In the present case, the compressive strain obtained from lattice constant values increases from 1.47×10^{-3} for $x = 0.1$ composition to 3.56×10^{-3} for $x = 0.2$ composition. Thus, the lattice potential energy decreases with increasing Ca^{2+}- substitution in the system. The same is the case with dislocation density obtained from grain size values. The dislocation density increases from 4.2×10^{-14} m^{-2} for $x = 0.0$ composition to 9.7×10^{-14} m^{-2} for $x = 1.0$ composition and as a result lattice potential energy is expected to decrease with ca-substitution. All such empirical parameters are not included in theoretical models employed in the present investigation, for the determination of lattice potential energy of ionic crystals. These lead to observed differences in the magnitude of lattice energy values.

4. Conclusion

The applicability of an experimental approach and five theoretical models in evaluating the lattice energies of oxide

Table 8. Lattice energies (U_{LS}) for $Ca_{1+x}Cu_{3-x}Ti_4O_{12}$ perovskite series from oxide additivity rule.

Ca^{2+}- concentration (x)	$-U_{LS}$ (eV)
0.0	660.87
0.1	660.19
0.2	659.52
0.5	657.50
1.0	654.14

compounds in multi-crystalline and mono-crystalline forms respectively is the highlight of the present investigation. With the anticipated difference, the theoretically estimated values of lattice energy for mono-crystalline counterparts have a good analogy with the experimentally determined values for polycrystalline materials. The change in inter-atomic distances and electronic configuration are governing parameters for the reduction in inter-atomic bonding strength and lattice energy values with Ca^{2+} substitution in the series, $Ca_{1+x}Cu_{3-x}Ti_4O_{12}$. This also suggests some sort of distortion from structural stability on Ca^{2+} substitution. Besides, contributions from grain boundary and grain, pore morphology, and the subsistence and evolution of micro-cracks are principal factors for the lower values of lattice energy corresponding to multi-crystalline materials in contrast with mono-crystalline counterparts. The lattice potential energy of constituent oxides can be used to ascertain the lattice energy of complex oxide systems.

Acknowledgment

The research fellowship given to N. S. Kanani under SHODH by the Government of Gujarat is highly appreciated.

Authors Contribution

All authors contributed to the study conception and design. The preparation of materials and primary characterization were carried out by D. K. Thummar and N. S. Kanani. The analysis of different models were carried out by D. J. Parekh and N. H. Vasoya. The manuscript was written, edited and finalized by K. B. Modi.

Availability of data and materials

The data that support the findings of this study are available from the corresponding author, upon reasonable request.

Conflict of interests

The authors declare that they have no known competing financial interests or personal relationships that could have appeared to influence the work reported in this paper.

References

[1] D. V. Barad, U. M. Meshiya, N. P. Joshi, P. L. Mange, P. Y. Raval, S. Kumar, et al. "Cation distribution and magnetic ordering evolution study on $Ca_{1+x}Cu_{3-x}Ti_4O_{12}$ ($x = 0.0$–0.2) perovskites. ". *Solid State Sci.*, **99**:106070, 2020.
DOI: https://doi.org/10.1016/j.solidstatesciences.2019.106070.

[2] D. V. Barad, P. L. Mange, K. K. Jani, S. Mukherjee, M. Ahmed, S. Kumar, et al. "Ca^{2+}- substitution effect on the defect structural changes in the quadruple perovskite series $Ca_{1+x}Cu_{3-x}Ti_4O_{12}$ studied by positron annihilation and complementary methods. ". *Ceram. Int.*, **47**:2631–2640, 2021.
DOI: https://doi.org/10.1016/j.ceramint.2020.09.110.

[3] P. Y. Raval, S. K. Modi, D. J. Parekh, N. P. Joshi, U. M. Meshiya, and K. B. Modi. "Enhancement in mechanical strength of Slow-Cooled quadruple perovskite $CaCu_3Ti_4O_{12}$ by microwave-assisted heating, and rapid thermal cooling process.". *Asian J. Adv. Res.*, **17**(1):14, 2022.
DOI: https://doi.org/10.1088/1674-4926/43/3/032001.

[4] D. J. Parekh, D. V. Barad, N. S. Kanani, D. K. Thummar, and K. B. Modi. "Influence of Ca^{2+}- substitution on elastic properties of $CaCu_3Ti_4O_{12}$ quadruple perovskite determined by ultrasonic pulse echo selection technique.". *Applied Radiation and Isotopes*, **60**:614–635, 2024.
DOI: https://doi.org/10.1134/S1061830924601545.

[5] T. Waddington. "Lattice energies and their significance in inorganic chemistry. ". *Advances in Inorganic Chemistry*, **1**:157–221, 1959.
DOI: https://doi.org/10.1016/S0065-2792(08)60254-X.

[6] A. F. Kapustinski. "Lattice energy of ionic crystals.". *Quart. Rev. Chem. Soc.*, **10**:455–628, 1971.

[7] H. D. B. Jenkins, D. Tudela, and L. Glasser. "Lattice potential energy estimation for complex ionic salts from density measurements.". *Inorg Chem.*, **41**:2364–2367, 2002.
DOI: https://doi.org/10.1021/ic011216k.

[8] L. Mu, C. Feng, and H. He. "Topological research on lattice energies for inorganic compounds. ". *MATCH Commun Math Comput Chem.*, **56**:97–111, 2006.
DOI: https://doi.org/10.1088/2516-1067/ab9d72.

[9] L. Glasser and H. D. B. Jenkins. "Ionic HydratesMpXq·nH_2O: Lattice energy and standard enthalpy of formation estimation. ". *Inorg. Chem.*, **122**:632–638, 2000.
DOI: https://doi.org/10.1021/ic020222t.

[10] S. Kaya and C. Kaya. "A simple method for the calculation of lattice energies of inorganic ionic crystals based on the chemical hardness.". *Inorg. Chem.*, **54**:8207–8213, 2015.
DOI: https://doi.org/10.1021/acs.inorgchem.5b00383.

[11] R. D. Shanon and G. R. Rossman. "Dielectric constants of silicate garnets and the oxide additivity rule. ". *Am. Min.*, **77**:94–100, 1992.

[12] A. K. Pandey, C. K. Dixit, and S. Srivastava. "Theoretical model for the prediction of lattice energy of diatomic metal halides.". *J. Maths. Chem.*, **62**:269–274, 2024.
DOI: https://doi.org/10.1007/s10910-023-01538-9.

[13] D. Liu, S. Zang, and Z. Wu. "Lattice energy estimation for inorganic ionic crystals. ". *Inorg. Chem.*, **42**:2465–2469, 2000.
DOI: https://doi.org/10.1021/ic025902a.

[14] S. Range, C. E. S. Bernardes, R. G. Simoes, M. Epple, and M. E. Minas de Piedade. "Size matters: An experimental and computational study of the influence of particle size on the lattice energy of NaCl.". *J. Phys. Chem. C.*, **199**:4387–4396, 2015.
DOI: https://doi.org/10.1021/jp5124772.

[15] S. Range, C. E. S. Bernardes, R. G. Simoes, M. Epple, and M. E. Minas de Piedade. "Size matters: An experimental and computational study of the influence of particle size on the lattice energy of NaCl.". *J. Phys. Chem. C.*, **199**:4387–4396, 2015.
DOI: https://doi.org/10.1021/jp5124772.

[16] M. R. Levy. "Crystal structure and defect property predictions in ceramic materials.". *Imperial College*, pages 79–144, 2005.

[17] K. B. Modi. "Lattice energy determination for polycrystalline oxide ceramics and single-crystalline counterparts. ". *J. Supercond. Nov. Magn.*, **29**:2287–2297, 2016.
DOI: https://doi.org/10.1007/s10948-016-3591-2.

[18] P. Zang, Y. Zhao, and W. Haito. "Bond ionicity, lattice energy, bond energy and microwave dielectric properties of ZnZr $(Nb_{1-x}A_x)_2O_8$ (A = Ta, Sb) ceramics. ". *Dalton. Trans.*, **44**:16684–16693, 2015.
DOI: https://doi.org/10.1039/C5DT02164B.

[19] P. Zhang, Y. Zhao, and X. Wang. "The relationship between bond ionicity, lattice energy, coefficient of thermal expansion and microwave dielectric properties of Nb $(Nb_{1-x}Sb_x)O_4$ ceramics.". *Dalton Trans.*, **44**:10932–10938, 2015.
DOI: https://doi.org/10.1039/C5DT01343G.

[20] M. Xiao, H. Sun, Z. Zhou, and P. Zhang. "Bond ionicity, lattice energy, bond energy, and microwave dielectric properties of $Ca_{1-x}Sr_xWO_4$ ceramics.". *Ceram. Int.*, **44**:20686–20691, 2018.
DOI: https://doi.org/10.1016/j.ceramint.2018.08.062.

[21] M. Xiao, Y. Wei, Q. Gu, Z. Zhou, and P. Zhang. "Relationships between bond ionicity, lattice energy, bond energy and the microwave dielectric properties of $La(Nb_{1-x}Ta_x)O_4$ ($x = 0 - 0.10$) ceramics.". *J. Alloys Compd.*, **775**:167–174, 2019.
DOI: https://doi.org/10.1016/j.jallcom.2018.09.304.

[22] M. Xiao, S. He, J. Meng, and P. Zhang. "Bond ionicity, lattice energy, bond energy and the microwave dielectric properties.". *Mater. Chem. Phys.*, **242**:122412, 2019.
DOI: https://doi.org/10.1016/j.matchemphys.2019.122412.

[23] P. Zhang, Y. Zhao, and L. Li. "The correlations among bond ionicity, lattice energy and microwave dielectric properties of $(Nd_{1-x}La_x)NbO_4$ ceramics. ". *Phys. Chem. Chem. Phys.*, **17**:16692–16698, 2015.
DOI: https://doi.org/10.1039/C5CP02204E.

[24] M. Xiao, Y. Wei, Q. Gu, and P. Zhang. "The relationship between the bond ionicity, lattice energy, bond energy and microwave dielectric properties of $LaNbO_4$ ceramics.". *J Mater Sci Mater Electro*, **9**: 9963–9970, 2018.
DOI: https://doi.org/10.1007/s10854-018-9038-8.

[25] X-Q. Song, W-Z. Lu, Y-H. Lou, T. Chen, S-W. Ta, Z-X. Fu, and W. Lei. "Synthesis, lattice energy and microwave dielectric properties of $BaCu_{2-x}Co_xSi_2O_7$ ceramics. ". *J. Euro. Ceram. Soc.*, **40**:3035–3041, 2020.
DOI: https://doi.org/10.1016/j.jeurceramsoc.2020.02.048.

[26] Y. Chen, S. Zhang, H. Yang, Y. Yuan, and E. Li. "Bond ionicity, lattice energy and structural evolution of Ta substituted 0.15ZnO-$0.15Nb_2O_5$-$0.55TiO_2$ dielectric ceramics.". *Ceram. Int.*, **45**:8832–8839, 2019.
DOI: https://doi.org/10.1016/j.ceramint.2019.01.210.

[27] X-Q. Song, W-Z. Lu, Y-H. Zou, T. Chen, S-W. Ta, Z-X. Fu, and W. Lei. "Crystal structure, lattice energy and microwave dielectric properties of melilite-type $Ba_{1-x}Sr_xCu_2Si_2O_7$ solid solutions.". *J. Alloys Compd.*, **835**:155340, 2020.
DOI: https://doi.org/10.1016/j.jallcom.2020.155340.

[28] L. Huang, Y. Li, F. Meng, L. Guo, Y. Liamg, Le. Zhang, X. Chen, B. Feng, K. Chen, Q. Zhang, L. Gu, J. Liu, and J. Zhu. "Disorder-insensitivity of room temperature gint permittivity in $Ca_{4-x}Cu_xTi_4O_{12}$ ($x = 3$, 2, and 1) polycrystalline ceramics. ". *J. Appl. Phys.*, **126**(6):224102, 2019.
DOI: https://doi.org/10.1063/1.5126348.

[29] M. A. Ramirez, P. R. Bueno, E. Longo, and J. A. Varela. "Conventional and microwave sintering of $CaCu_2Ti_4O_{12}$/$CaTiO_3$ ceramic composites, non-ohmic and dielectric properties. ". *J. Phys. D.: Appl. Phys.*, **41**:152004, 2008.
DOI: https://doi.org/10.1088/0022-3727/41/5/152004.

[30] K. K. Jani, D. V. Barad, P. Y. Raval, M. Nehra, N. H. Vasoya, N. Jakhar, et al. "Ca^{2+}- substitution effect on the electronic structure of $CaCu_3Ti_4O_{12}$ studied by electron spectroscopy for chemical analysis.". *Ceram Int.*, **47**:5542–5548, 2021.
DOI: https://doi.org/10.1016/j.ceramint.2020.10.138.

[31] B. R. Reddy and N. Harikumar. "Effect of Bi_2O_3 and sintering temperature on the ultrasonic properties of Mn-Zn Ferrite. ". *Int. J. Sci. Res.*, **3**:1820, 2014.

[32] V. K. Lakhani and K. B. Modi. "Al^{3+} modified elastic properties of copper ferrites.". *Solid State Sci.*, **12**:2134–2143, 2010.
DOI: https://doi.org/10.1016/j.solidstatesciences.2010.09.012.

[33] P. U. Sharma and K. B. Modi. "Effect of Fe^{3+} substitution on elastic properties of yttrium iron garnet.". *Phys. Scr.*, **81**:015601, 2010.
DOI: https://doi.org/10.1088/0031-8949/81/01/015601.

[34] B. B. Kudriastev. "Lattice energy determination for polycrystalline oxide ceramics and single-crystalline counterparts". *Applied Radiation and Isotopes*, **29**:2287–2297, 1956.
DOI: https://doi.org/10.1007/s10948-016-3591-2.

[35] K. B. Modi, S. J. Shah, T. K. Pathak, N. H. Vasoya, V. K. Lakhani, and A. K. Yahya. "Improvement in elastic properties of $CuAl_{0.4}Fe_{1.6}O_4$ spinel.". *AIP Conf. Proc.*, **1591**:1115–1117, 2014.
DOI: https://doi.org/10.1063/1.4872872.

[36] K. B. Modi, S. J. Shah, N. B. Pujara, T. K. Pathak, N. H. Vasoya, and I. G. Jhala. "Infrared spectral evolution, elastic, optical and thermodynamic properties study on mechanically milled $Ni_{0.5}Zn_{0.5}Fe_2O_4$ spinel ferrite.". *J. Mol. Struc.*, **1049**:250–262, 2013.
DOI: https://doi.org/10.1016/j.molstruc.2013.06.051.

[37] J. J. U. Buch, G. Lalitha, T. K. Pathak, N. H. Vasoya, V. K. Lakhani, P. V. Reddy, et al. "Structural and elastic properties of Ca-substituted $LaMnO_3$ at 300 K.". *J. Phys. D Appl. Phys.*, **41**:025406, 2008.
DOI: https://doi.org/10.1088/0022-3727/41/2/025406.

[38] M. B. Solunke, K. B. Modi, V. K. Lakhani, K. B. Zankat, P. U. Sharma, P. V. Reddy, et al. "Effect of Ag^+-addition on elastic behaviour of Bi-2212 superconductors. ". *Ind. J. Pure Appl. Phys.*, **45**:764–766, 2007. URL http://nopr.niscpr.res.in/handle/123456789/2665.

[39] R. Rajmi, A. K. Yahya, and M. I. M. Yusuf. "Effect of $MgTiO_3$ Doping on Dielectric and Elasticity Properties of $CaCu_3Ti_4O_{12}$. ". *Aust J Basic Appl Sci.*, **5**:405–416, 2011.

[40] F. de Boer, J. H. van Santen, and E. J. W. Verway. "The electrostatic contribution to the lattice energy of some ordered spinels.". *J. Chem. Phys.*, **18**:1032, 1950.
DOI: https://doi.org/10.1063/1.1747852.

[41] G. C. Mather, M. S. Islam, and F. M. Figueiredu. "Atomistic study of a $CaTiO_3$-based mixed conductor: Defects, nanoscale clusters, and oxide-ion migration. ". *Adv. Funct. Mater.*, **17**:905–912, 2007.
DOI: https://doi.org/10.1002/adfm.200600632.

[42] H. Donnerberg and C. R. A. Catlow. "Atomistic computer simulations of yttrium iron garnet (YIG) as an approach to materials defect.". *J. Phys. Cond. Matter.*, **5**:2947–2960, 1993.
DOI: https://doi.org/10.1088/0953-8984/5/18/017.

[43] R. M. Dreizler and E. K. U. Gross. "Density Function Theory. ". *Springer*, pages 245–271, 1990.
DOI: https://doi.org/10.1007/978-3-642-86105-5_8.

[44] P. K. Chattaraj, S. Giri, and S. J. Duley. "Aromaticity and conceptual density functional theory.". *Applied Radiation and Isotopes*, **1**:1064, 2010.
DOI: https://doi.org/10.1039/9781849732789-00045.

[45] W. D. Callister. "Materials science and engineering: an introduction. ". *Springer*, **80**, 2000.
DOI: https://doi.org/10.1557/PROC-760-JJ6.1.

[46] F. Mikailzade, F. Önal, M. Maksutoglu, M. Zarbali, and A. Goktas. "Structure and magnetization of polycrystalline $La_{0.66}Ca_{0.33}MnO_3$ and $La_{0.66}Ba_{0.33}MnO_3$ films prepared using Sol-Gel technique.". *J. Supercond. Nov. Magn*, **31**:4141–4145, 2018.
DOI: https://doi.org/10.1007/s10948-018-4683-y.

[47] M. Shi, S. Ma, W. Xia, Y. Wang, J. Yu, and H. Wu. "Effect of oxygen vacancy on bond iconicity , lattice energy , and microwave dielectric properties of CeO_2 ceramics with Yb^{3+} substitution.". *J. Adv. Ceram.*, **13**:247–254, 2024.
DOI: https://doi.org/10.26599/JAC.2024.9220848.

[48] A. Goktas, I. H. Mutlu, and A. Kawashi. "Growth and characterization of $La_{1-x}A_xMnO_3$ (A = Ag and K, $x = 0.33$) epitaxial and polycrystalline manganite thin films derived by sol–gel dip-coating technique. ". *Thin Solid Films*, **520**:6138–6144, 2012.
DOI: https://doi.org/10.1016/j.tsf.2012.06.006.